

Electronic Supplementary Information (ESI)

Interesting dimensional transition through changing cations as the trigger in multinary thioarsenates displaying variable photocurrent response and optical anisotropy

Chao Zhang,^a Sheng-Hua Zhou,^{b,c,d} Yu Xiao,^a Hua Lin,^{*,b,c,d} and Yi Liu^{*,a}

^a*Institute for Composites Science Innovation (InCSI), School of Materials Science and Engineering, Zhejiang University, Hangzhou 310027, China*

^b*State Key Laboratory of Structural Chemistry, Fujian Institute of Research on the Structure of Matter, Chinese Academy of Sciences, Fuzhou 350002, China*

^c*Fujian Science & Technology Innovation Laboratory for Optoelectronic Information of China, Fuzhou 350108, China*

^d*University of Chinese Academy of Sciences, Beijing 100049, China*

*E-mail: liuyimse@zju.edu.cn and linhua@fjirsm.ac.cn.

Electronic Supplementary Information Index

1. Experimental Section

1.1 Physical Measurements

1.2 Syntheses of Cs₂ZnAs₄S₈ and [(NH₄)Cs]CdAs₄S₈

1.3 Single-Crystal Structure Characterizations

2. Computational Details

3. Figures and Tables

Figure S1. The coordination environment of crystallographic unique Cs atoms in (a) Cs₂ZnAs₄S₈ and (b) [(NH₄)Cs]CdAs₄S₈.

Figure S2. SEM image and energy-dispersive X-ray spectroscopy analysis of Cs₂ZnAs₄S₈.

Figure S3. SEM image and energy-dispersive X-ray spectroscopy analysis of

$[(\text{NH}_4)\text{Cs}]\text{CdAs}_4\text{S}_8$.

Figure S4. Experimental (black solid line), calculated (red cross), positions of the Bragg peaks (vertical bars) and difference (blue) results of powder XRD refined by General Structure Analysis System (GSAS) for as-synthesized $\text{Cs}_2\text{ZnAs}_4\text{S}_8$.

Figure S5. Experimental (black solid line), calculated (red cross), positions of the Bragg peaks (vertical bars) and difference (blue) results of powder XRD refined by General Structure Analysis System (GSAS) for as-synthesized $[(\text{NH}_4)\text{Cs}]\text{CdAs}_4\text{S}_8$.

Figure S6. TG-DTA diagrams of $\text{Cs}_2\text{ZnAs}_4\text{S}_8$.

Figure S7. TG-DTA diagrams of $[(\text{NH}_4)\text{Cs}]\text{CdAs}_4\text{S}_8$.

Table S1. Selected bond lengths (Å) for $\text{Cs}_2\text{ZnAs}_4\text{S}_8$ and $[(\text{NH}_4)\text{Cs}]\text{CdAs}_4\text{S}_8$.

4. References

1. Experimental Section

Physical Measurements. The elemental analyses have been examined with via an EDX-equipped JEOL/JSM-6360A SEM. Powder X-ray diffraction data were collected on a Bruker D8 Advance diffractometer with a graphite-monochromatized Cu K_{α} radiation and data were analyzed using a profile fitting by a least-squares method employing the computer program GSAS implemented with EXPGUI.¹ The operating 2θ angle ranges from 10° to 80° . Simulation of XRD patterns were carried out by the single-crystal data and diffraction-crystal module of the Mercury (Hg) program version 1.4.2 available free of charge through the website <http://www.iucr.org>. The optical diffuse reflectance spectra were measured on a Hitachi UH4150 UV–vis-NIR spectrometer equipped with an integrating sphere at room temperature. The picked polycrystalline samples were ground into fine powders before measurement. The absorption (α/S) data were calculated from reflectance with the Kubelka–Munk function: $\alpha/S = (1-R)^2/2R$, in which α is the absorption coefficient, R is the reflectance at a specified wavelength, and S is the scattering coefficient.² The photo-electrochemical tests were done under simulated solar light illumination using an electrochemical workstation (CHI660E) with conventional three-electrode setup on open circuit voltage. Each as-prepared powder sample was coated onto a slice of ITO glass with an area of $0.5 \times 1 \text{ cm}^2$ and employed as the working electrode. A saturated Hg/Hg₂Cl₂ and a platinum wire were used as the reference and counter electrodes, respectively, and 0.2 M Na₂SO₄ aqueous solution with 10% lactic acid was used as electrolyte. A 500 W Xe lamp was utilized as the simulated solar light source.

Syntheses of $\text{Cs}_2\text{ZnAs}_4\text{S}_8$ and $[(\text{NH}_4)\text{Cs}]\text{CdAs}_4\text{S}_8$. The starting reagents $\text{CsOH}\cdot\text{H}_2\text{O}$ (99.7%), Zn powder (99.7%), S powder (99.5%) and hydrazine monohydrate (85%) purchased from Sinopharm Chemical Reagent Co., Ltd. were used as obtained. Oleic acid (85%) and the binary starting material As_2S_3 (99.9%) was purchased from Aladdin Co., Ltd. All the chemicals used for synthesis are of analytical grade and directly used without further purification.

Compound $\text{Cs}_2\text{ZnAs}_4\text{S}_8$ was obtained by the reaction as follows: 1.5 mmol of $\text{CsOH}\cdot\text{H}_2\text{O}$, 0.4 mmol of Zn, 0.5 mmol of As_2S_3 , 2.5 mmol of S, 2.0 mL of oleic acid and 0.5 mL of hydrazine monohydrate. All reactants were sealed in a 25 mL Teflon-lined stainless autoclave which was kept at 413 K for 7 days prior to cooling to room temperature naturally. The resultant reaction mixtures were washed with distilled water and ethanol, respectively. A lot of yellow block-shaped $\text{Cs}_2\text{ZnAs}_4\text{S}_8$ crystals (approximately 90% yield based on Zn) were obtained and pure phase could be easily obtained by manually picking crystals from the mixtures.

Compound $[(\text{NH}_4)\text{Cs}]\text{CdAs}_4\text{S}_8$ was synthesized with similar procedures. A lot of orange block-shaped $[(\text{NH}_4)\text{Cs}]\text{CdAs}_4\text{S}_8$ crystals (approximately 80% yield based on Cd) were obtained. Both $\text{Cs}_2\text{ZnAs}_4\text{S}_8$ and $[(\text{NH}_4)\text{Cs}]\text{CdAs}_4\text{S}_8$ are stable in air for several months. Their phase purities have been confirmed by the powder XRD patterns matching well with the simulated ones.

Single-Crystal Structure Characterizations. Suitable single crystals of the title compounds were mounted on the glass fibers. Diffraction data were collected by an Oxford Xcalibur (Atlas Gemini ultra) diffractometer with a graphite-monochromated

Mo-K α radiation ($\lambda = 0.71073 \text{ \AA}$) at room temperature. The absorption corrections were based on the multi-scan method. The structures were solved by the direct methods and refined by the full-matrix least-squares fitting on F^2 using the *SHELXL-2014* software package.³ The assignments of atoms were determined on the basis of the interatomic distances, coordination environments and relative displacement parameters. The structure was verified using the *ADDSYM* algorithm from the program *PLATON*.⁴ The final atomic positions were standardized with the *STRUCTURE TIDY* program.⁵ Crystal data and refinement details are summarized in Tables 1-2, the selected bond lengths are listed in Table S1. CCDC number: 2167064–2167065.

Computational Details. Crystallographic data determined by single crystal X-ray diffraction were used for theoretical calculations of their electronic band structures. The density functional theory (DFT) calculations have been performed using the Vienna ab initio simulation package (VASP)⁶⁻⁸ with the Perdew-Burke-Ernzerhof (PBE)⁹ exchange correlation functional. The projected augmented wave (PAW)¹⁰ potentials have been used to treat the ion-electron interactions. A Γ -centered $5 \times 5 \times 7$ Monkhorst-Pack grid for the Brillouin zone sampling and a cutoff energy of 700 eV for the plane wave expansion were found to get convergent lattice parameters and self-consistent energies.

Figures and Tables

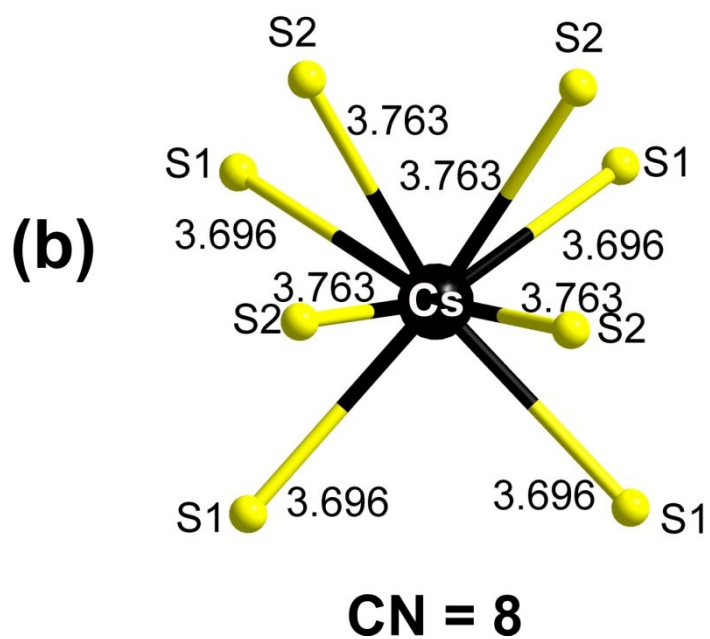
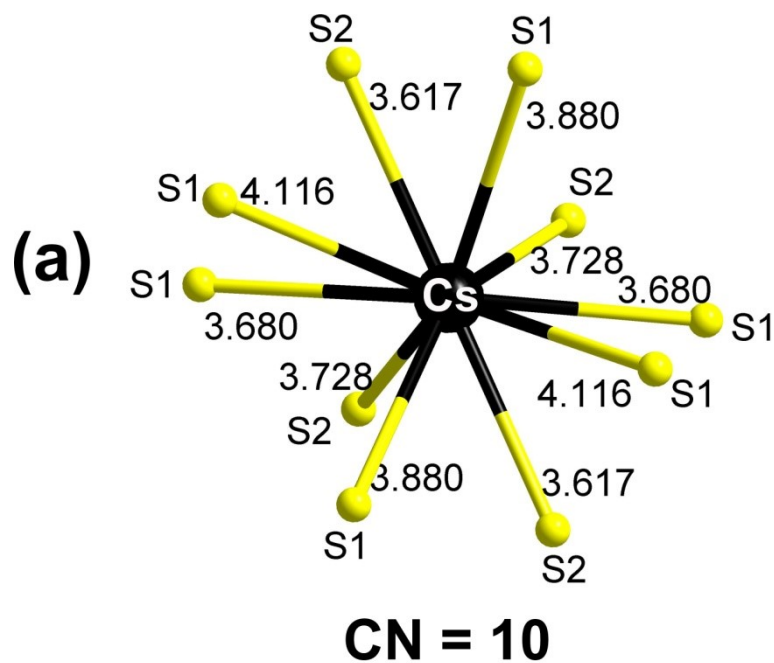


Figure S1. The coordination environment of crystallographic unique Cs atoms in (a) $\text{Cs}_2\text{ZnAs}_4\text{S}_8$ and (b) $[(\text{NH}_4)\text{Cs}]\text{CdAs}_4\text{S}_8$.

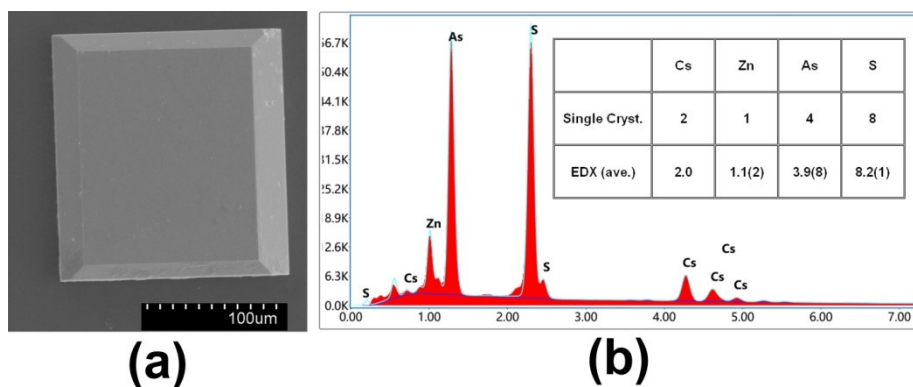


Figure S2. SEM image and energy-dispersive X-ray spectroscopy analysis of $\text{Cs}_2\text{ZnAs}_4\text{S}_8$.

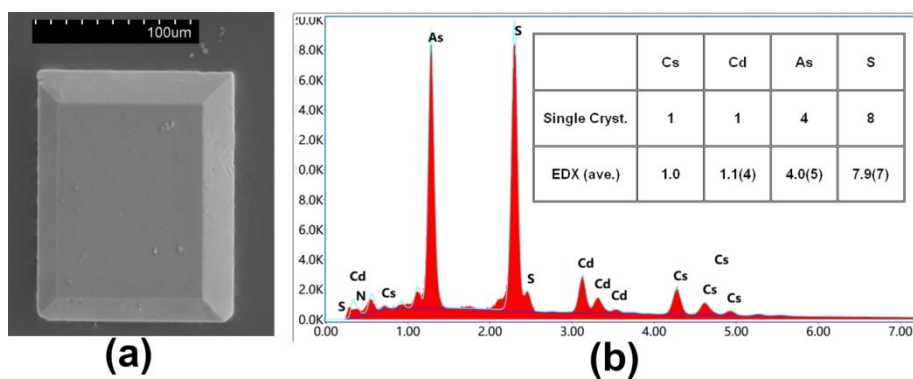


Figure S3. SEM image and energy-dispersive X-ray spectroscopy analysis of $[(\text{NH}_4)\text{Cs}]\text{CdAs}_4\text{S}_8$.

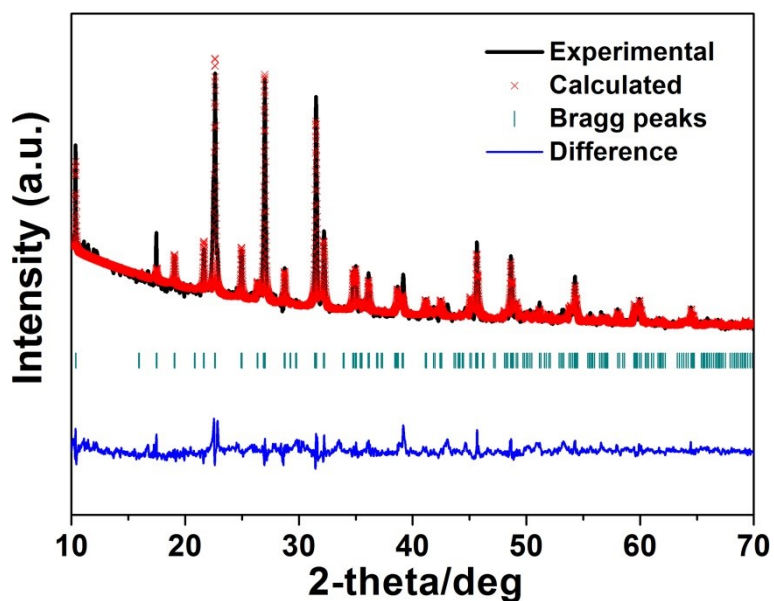


Figure S4. Experimental (black solid line), calculated (red cross), positions of the Bragg peaks (vertical bars) and difference (blue) results of powder XRD refined by General Structure Analysis System (GSAS) for as-synthesized $\text{Cs}_2\text{ZnAs}_4\text{S}_8$.

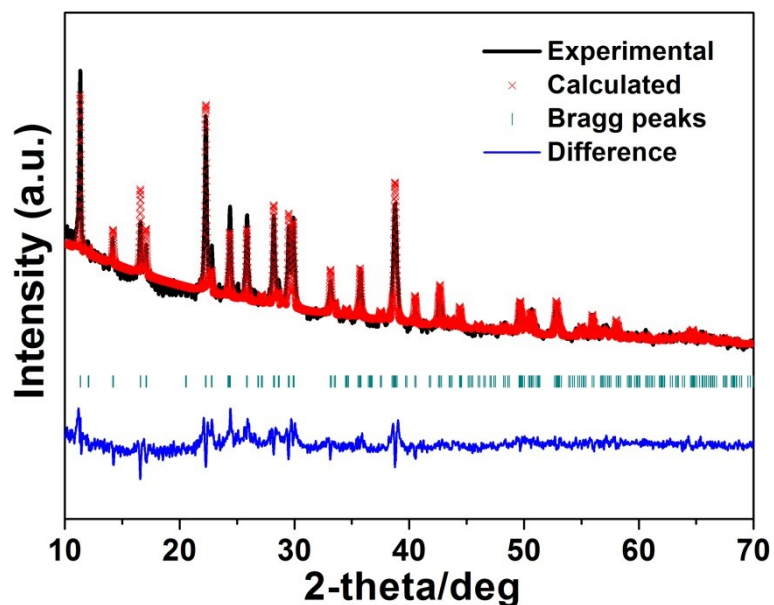


Figure S5. Experimental (black solid line), calculated (red cross), positions of the Bragg peaks (vertical bars) and difference (blue) results of powder XRD refined by General Structure Analysis System (GSAS) for as-synthesized $[(\text{NH}_4)\text{Cs}]\text{CdAs}_4\text{S}_8$.

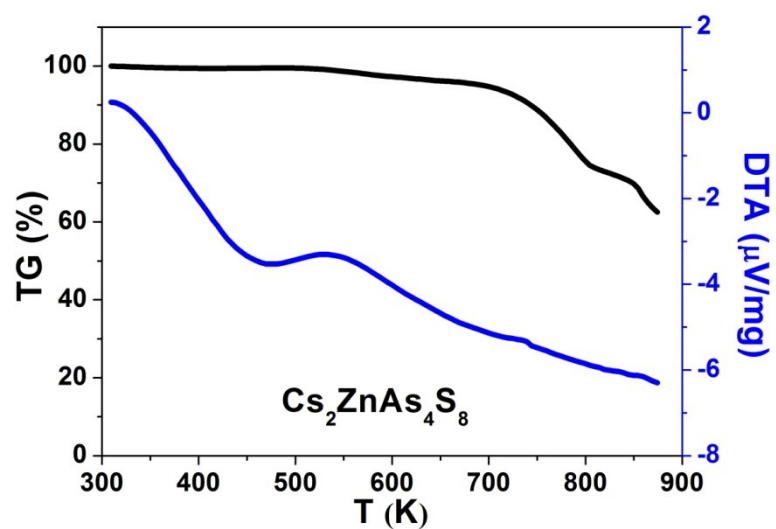


Figure S6. TG-DTA diagrams of $\text{Cs}_2\text{ZnAs}_4\text{S}_8$.

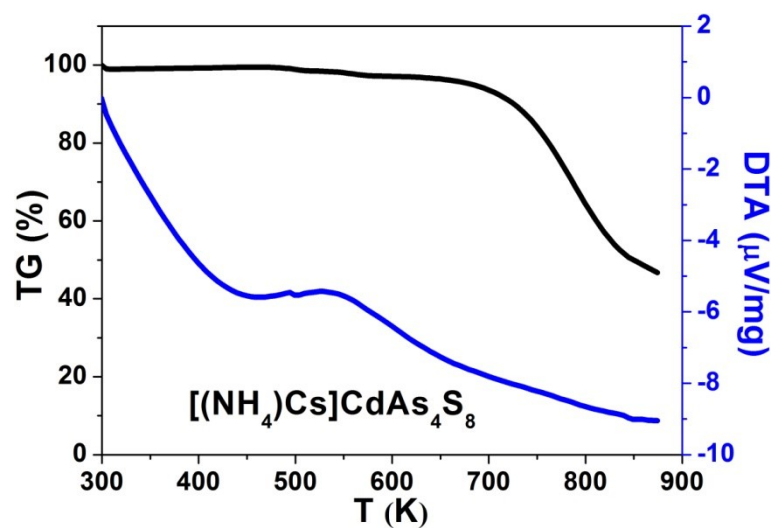


Figure S7. TG-DTA diagrams of $[(\text{NH}_4)\text{Cs}]\text{CdAs}_4\text{S}_8$.

Electronic Supplementary Information (ESI)

Table S1. Selected bond lengths (Å) for Cs₂ZnAs₄S₈ and [(NH₄)Cs]CdAs₄S₈.

Cs ₂ ZnAs ₄ S ₈		[(NH ₄)Cs]CdAs ₄ S ₈	
As–S2	2.2143(5)	As–S1	2.2086(5)
As–S1	2.2738(5)	As–S2	2.2676(5)
As–S1	2.3267(5)	As–S2	2.3008(5)
Zn–S2 ×4	2.3309(5)	Cd–S1 ×4	2.5481(5)
Cs–S2	3.6170(5)	Cs–S1 ×4	3.6957(5)
Cs–S1	3.6810(6)	Cs–S2 ×4	3.7634(5)
Cs–S2	3.7277(5)		
Cs–S1	3.8795(5)		
Cs–S1	4.1160(6)		
∠S2–As–S1	94.17(2)	∠S1–As–S2	99.315(18)
∠S2–As–S1	103.280(19)	∠S1–As–S2	99.650(18)
∠S1–As–S1	98.074(13)	∠S1–As–S2	101.38(2)
∠S2–Zn–S2 ×4	105.787(11)	∠S1–Cd–S1 ×4	106.820(10)
∠S2–Zn–S2 ×2	117.12(2)	∠S1–Cd–S1 ×2	114.91(2)

4. References

- (1) B. H. Toby, *EXPGUI, a graphical user interface for GSAS. J. Appl. Crystallogr.*, 2001, **34**, 210.
- (2) G. Kortüm, *Reflectance Spectroscopy*; Springer-Verlag: New York, 1969.
- (3) Sheldrick, G. M. A short history of SHELX, *Acta Crystallogr., Sect. A: Found. Crystallogr.*, 2008, 112–122.
- (4) A. L. Spek, Single-crystal structure validation with the program PLATON, *J. Appl. Cryst.*, 2003, **36**, 7–13.
- (4) L. M. Gelato and E. J. Parthe, STRUCTURE TIDY—a computer program to standardize crystal structure data, *Appl. Crystallogr.*, 1987, **20**, 139–143.
- (5) M. D. Segall, P. J. D. Lindan, M. J. Probert, C. J. Pickard, P. J. Hasnip, S. J. Clark and M. C. Payne, First-principles simulation: ideas, illustrations and the CASTEP code, *J. Phys.: Condens. Matter*, 2002, **14**, 2717–2744.
- (6) G. Kresse, VASP, 5.3.5; <http://cms.mpi.univie.ac.at/vasp/vasp/vasp.html>.
- (7) G. Kresse and J. Furthmüller, Efficient iterative schemes for ab initio total-energy calculations using a plane-wave basis set, *Phys. Rev. B: Condens. Matter*, 1996, **54**, 11169–11186.
- (8) G. Kresse and D. Joubert, From ultrasoft pseudopotentials to the projector augmented-wave method, *Phys. Rev. B: Condens. Matter*, 1999, **59**, 1758–1775.
- (9) J. P. Perdew, K. Burke and M. Ernzerhof, Generalized gradient approximation made simple, *Phys. Rev. Lett.*, 1996, **77**, 3865–3868.
- (10) P. E. Blochl, Projector augmented-wave method, *Phys. Rev. B: Condens. Matter*,

Electronic Supplementary Information (ESI)

1994, **50**, 17953–17979.